

Dependence of Excited State Potential Energy Surfaces on the Spatial Overlap of the Kohn–Sham Orbitals and the Amount of Nonlocal Hartree–Fock Exchange in Time-Dependent Density Functional Theory

Jürgen Plötner,[†] David J. Tozer,[‡] and Andreas Dreuw^{*,†}

Institute of Physical and Theoretical Chemistry, Goethe-University Frankfurt, Max von Laue-Strasse 7, 60438 Frankfurt, Germany, and Department of Chemistry, University of Durham, South Road, Durham DH1 3LE, United Kingdom

Received April 13, 2010

Abstract: Time-dependent density functional theory (TDDFT) with standard GGA or hybrid exchange-correlation functionals is not capable of describing the potential energy surface of the S_1 state of Pigment Yellow 101 correctly; an additional local minimum is observed at a twisted geometry with substantial charge transfer (CT) character. To investigate the influence of nonlocal exact orbital (Hartree–Fock) exchange on the shape of the potential energy surface of the S_1 state in detail, it has been computed along the twisting coordinate employing the standard BP86, B3LYP, and BHLYP xc-functionals as well as the long-range separated (LRS) exchange-correlation (xc)-functionals LC-BOP, ω B97X, ω PBE, and CAM-B3LYP and compared to RI-CC2 benchmark results. Additionally, a recently suggested Λ -parameter has been employed that measures the amount of CT in an excited state by calculating the spatial overlap of the occupied and virtual molecular orbitals involved in the transition. Here, the error in the calculated S_1 potential energy curves at BP86, B3LYP, and BHLYP can be clearly related to the Λ -parameter, i.e., to the extent of charge transfer. Additionally, it is demonstrated that the CT problem is largely alleviated when the BHLYP xc-functional is employed, although it still exhibits a weak tendency to underestimate the energy of CT states. The situation improves drastically when LRS-functionals are employed within TDDFT excited state calculations. All tested LRS-functionals give qualitatively the correct potential energy curves of the energetically lowest excited states of P. Y. 101 along the twisting coordinate. While LC-BOP and ω B97X overcorrect the CT problem and now tend to give too large excitation energies compared to other non-CT states, ω PBE and CAM-B3LYP are in excellent agreement with the RI-CC2 results, with respect to both the correct shape of the potential energy curve as well as the absolute values of the calculated excitation energies.

Introduction

During the last 25 years, linear-response time-dependent density functional theory (TDDFT)^{1–3} has become one of the most widely used quantum chemical methods to study excited electronic states of medium sized to large molecules

with say 30 up to 300 second row atoms. (See, for example, refs 4–7.) In general, locally excited electronic states that lie energetically well below the ionization potential, e.g., typical $\pi\pi^*$ or $n\pi^*$ transitions, are usually well described within TDDFT using standard exchange-correlation (xc)-functionals, very often with accuracies close to those of sophisticated wave function based methods. Typically, these $\pi\pi^*$ excited states carry most of the oscillator strength, and thus, experimental absorption spectra are very often ac-

* Corresponding author e-mail: andreas@theochem.uni-frankfurt.de.

[†] Goethe-University Frankfurt.

[‡] University of Durham.

curately reproduced.^{8,9} The excellent cost-to-accuracy relationship that TDDFT offers for the calculation of such experimental spectra is the basis for the great early success of TDDFT.

In contrast, charge transfer (CT) excited states are often described very poorly using standard local xc-functionals.^{10–13} In principle, these states suffer from two related deficiencies of the standard functionals. On one hand, so-called electron transfer self-interaction is not correctly eliminated by the response of local xc-potentials leading to a physically incorrect asymptotic behavior of the potential energy curves with respect to a separation coordinate of the generated positive and negative (partial) charges in a CT excited state.^{3,11,12} Second, the excitation energies tend to be significantly underestimated, which can be related to the integer discontinuity¹⁴ in the case of asymptotic intermolecular excitations.¹⁵ It was recognized very early that these failures are related to the locality of the employed xc-potentials and the inclusion of long-range, nonlocal exact orbital (Hartree–Fock) exchange would alleviate these problems.¹¹ Along these lines of thought, several long-range separated xc-potentials have been proposed, e.g., CAM-B3LYP,¹⁶ LC-BLYP or LC-BOP,^{17–19} ω PBE,^{20,21} ω B97x,^{22,23} LC- ω PBE,^{24,25} and others,^{26,27} and it has been demonstrated that these functionals indeed improve the description of CT excited states in TDDFT substantially. Also, the application of exact local Kohn–Sham exchange^{28,29} instead of nonlocal Hartree–Fock exchange is a viable route to overcome the CT problem as first tests have recently shown.³⁰

However, a potential problem of the inclusion of long-range Hartree–Fock (HF) exchange into TDDFT is the corruption of its well-known accuracy for locally excited states described above. This relates to the fact that Hartree–Fock exchange leads to an increase of the energy gap between the occupied and virtual orbitals owing to Koopmans' Theorem, making virtual-occupied orbital energy differences a poor zeroth order estimate for excitation energies. Therefore, it is not always useful or desirable to turn to long-range separated xc-functionals, and instead, one may wish to stay with the standard xc-functionals. In such situations, it is very important to possess a diagnostic tool to estimate the influence of the CT failure, i.e., to judge the expected quality of the computed excitation energies and as such the usefulness of the chosen xc-functional for the molecular system under consideration.

It is clear that the error in excitation energies due to the CT failure depends on the extent of charge transfer, and therefore, one should aim at measuring the degree of CT in a particular excited state. An intuitive measure of charge transfer character is given by the spatial overlap of the electron donating orbitals and the electron accepting orbitals.³¹ In an excited state, the former are given by the occupied orbitals that are depopulated upon excitation while the latter correspond to the virtual orbitals that get populated. Peach et al. have recently proposed such a CT measure, Λ as the sum of the spatial overlaps O_{ia} between occupied and virtual orbitals involved in one excited state weighted by the square of their transition amplitudes κ_{ia} ,³¹

$$\Lambda = \frac{\sum_{ia} \kappa_{ia}^2 O_{ia}}{\sum_{ia} \kappa_{ia}^2} \quad (1)$$

where the spatial overlap is given as

$$O_{ia} = \langle i | \varphi_i || \varphi_a \rangle = \int |\varphi_i(r)| |\varphi_a(r)| dr \quad (2)$$

It was clearly demonstrated that the parameter Λ correlates with the error in excitation energies, i.e., the smaller the Λ , the larger are both the CT character and the error.^{31–35}

In this contribution, we evaluate the performance of long-range separated functionals in the description of intramolecular charge transfer and, in addition, demonstrate the usefulness of the CT diagnostic Λ for the investigation of real photochemical problems. For that purpose, we reinvestigate the photochemistry of Pigment Yellow 101 (P. Y. 101, Figure 1), a commercially available fluorescent yellow pigment. Besides its fluorescence as the main excited state decay channel, P. Y. 101 exhibits a surprisingly rich photochemistry.^{8,36–38} Upon photoexcitation into the first excited S_1 state, different competing processes occur: excited state intramolecular proton transfer (ESIPT), isomerization at the central N–N bond and, of course, fluorescence. We have chosen P. Y. 101, since its vertical absorption spectrum is very nicely reproduced using TDDFT with the standard local BP86 xc-functional. However, on the other hand, it has been shown that the potential energy surface of the S_1 state exhibits an artificial minimum at a twisted geometry with a CNNC (C=N–N=C) dihedral angle of the central bisazomethine group of 90° at this level of theory adulterating the excited state dynamics.³⁸ This artificial minimum occurs due to the CT failure of TDDFT, since the increasing amount of CT character of the S_1 state along the twisting coordinate leads to a spurious lowering of the excited state energy. The same effect has also been observed for 4-(dimethylamino)benzonitrile.³⁴ In summary, P. Y. 101 is one example of those molecules where one rather sticks to the common local xc-functionals due to the high quality of the vertical description of the S_1 $\pi\pi^*$ state, but still, one needs a diagnostic tool to evaluate the quality of the potential energy surface along some reaction coordinate where the amount of CT character may increase. We will show here the parameter Λ is a suitable tool for that purpose.

The paper is organized as follows. In the following section, the computational details of our theoretical investigation will be outlined. Our results will be presented and discussed, first starting with benchmark calculations at the RI-CC2 level of theory, then turning to TDDFT results employing standard local and hybrid xc-functionals and the application of the CT measure Λ , and finally giving TDDFT results obtained using long-range separated xc-functionals. The paper concludes with a brief summary of the main conclusions.

Computational Details

The minimum energy pathway for excited state intramolecular proton transfer (ESIPT) of P. Y. 101 has been computed at the TDDFT/BP86/DZP, and it has been noted

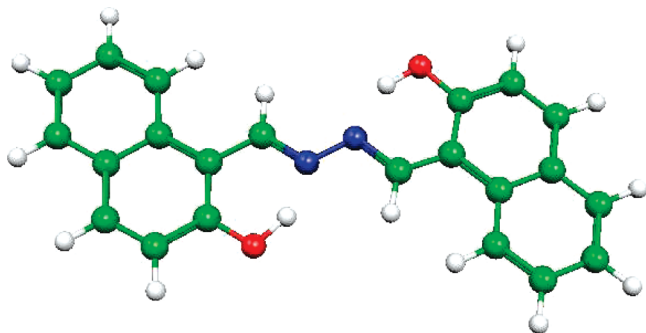


Figure 1. Molecular structure of Pigment Yellow 101.

previously that the central bisazomethine CNNC subunit supposedly twists upon proton transfer at that level of theory.³⁸ In fact, the minimum on the excited state potential energy surface corresponding to the twisted geometry of the keto-form of P. Y. 101 with a central CNNC dihedral angle of almost 90° is an artifact of the employed BP86 xc-functional and originates most likely from the CT failure. Therefore, we focus here on the twisting of the keto-form of P. Y. 101 only, and the C=N–N=C dihedral angle is scanned from 180° (planar keto-minimum) to 90° (twisted artificial minimum). The potential energy curves have been recomputed along this pathway at the TDDFT/BP86 optimized geometries using TDDFT with the standard B3LYP^{39,40} and BHLYP⁴¹ hybrid xc-functionals and with the newly developed long-range separated xc-functionals LC-BOP,^{17,18} ω PBE,^{20,21} and ω B97X^{22,23} as well as CAM-B3LYP¹⁶ using the standard 6-31G* basis set. In addition, the approximate coupled-cluster theory of second order exploiting the resolution-of-the-identity approximation (RI-CC2) has been used for benchmarking purposes.⁴² For the RI-CC2 calculations, the DZP basis set has been used along with the auxiliary SVP basis set for the density fitting, and the energetically sixteen lowest occupied molecular orbitals were frozen. The equations for the computation of the Λ parameter to measure the CT character of an excited state have been implemented into a development version of the Q-Chem 3.2 program package.⁴³ This code has been used to compute Λ for the lowest excited S_1 state of P. Y. 101 along the twisting coordinate for all xc-functionals employed in our TDDFT calculations. All calculations have been performed using the Turbomole 5.10 program package,⁴⁴ a development version of Q-Chem 3.2,⁴³ and the CAM-B3LYP calculations have been done with Dalton.⁴⁵

Twisting P. Y. 101 at the CC2 Level of Theory. To evaluate the performance of different xc-functionals in the computation of the potential energy surface of the S_1 electronic state of P. Y. 101 along the reaction coordinate representing the twisting of the central bisazomethine unit, we have first computed the five lowest excited states using RI-CC2 along the TDDFT/BP86 optimized reaction path. The obtained potential energy curves are displayed in Figure 2. The curve obtained for the S_1 state, which is responsible for the excited state dynamics of P. Y. 101, serves as benchmark for the evaluation of the quality of the TDDFT results with respect to the CT failure discussed in later sections. This is justified, since CC2 being an ab initio method does not suffer from the charge transfer failure and,

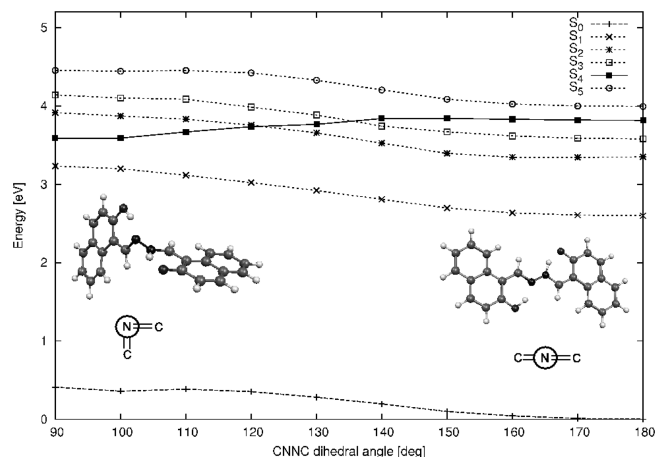


Figure 2. Potential energy curves of the ground and five lowest excited electronic states computed at the level of RI-CC2 along the twisting coordinate of the central bisazomethine subunit of the keto-form of P. Y. 101. In the insets, the planar (180°) and twisted (90°) structures as well as the corresponding Newman projections are also displayed.

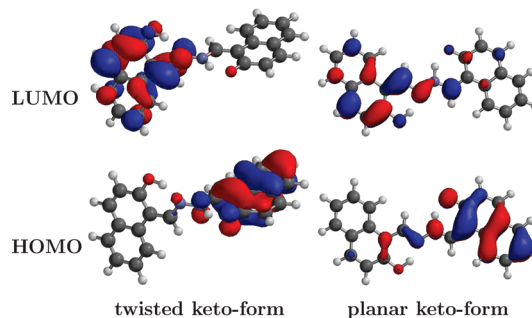


Figure 3. Highest occupied and lowest unoccupied molecular orbitals (HOMO and LUMO) at the theoretical level of Hartree–Fock for the planar and twisted keto-forms of P. Y. 101.

on the contrary, describes singly excited states with an accuracy comparable to EOM-CCSD, i.e., with an error of 0.1–0.3 eV.^{42,46}

While the planar keto-form of P. Y. 101 with a central CNNC dihedral angle of 180° corresponds to a true local minimum on the S_1 potential energy surface at the theoretical level of RI-CC2, the twisted form with a dihedral angle of 90° corresponds to a transition state connecting the trans and cis keto-isomers of P. Y. 101. At the theoretical level of RI-CC2, the twisted geometry lies 0.63 eV above the trans keto-minimum. Overall, the potential energy curve of the S_1 state follows the one of the electronic ground state along the investigated CNNC twisting coordinate. The barrier for twisting, however, is with 0.63 eV slightly higher in the S_1 state than in the ground state, where the barrier exhibits a value of 0.4 eV. In the molecular orbital picture, the S_1 electronic state is mainly characterized by a single excitation of an electron out of the highest occupied molecular orbital (HOMO) into the lowest unoccupied molecular orbital (LUMO), which are both displayed in Figure 3 for the planar as well as twisted geometries of the keto-form of P. Y. 101. As is easily seen, the bonding character of the N–N bond does slightly differ in the HOMO and the LUMO. While

the HOMO exhibits weak antibonding character along the N–N bond, the LUMO is weakly bonding explaining the small increase in the twisting barrier. Moreover, the HOMO and LUMO also reveal the charge transfer character of the S_1 state already in the planar trans keto-form, since the lobes of the two orbitals are located mainly on opposite rings. Going to the twisted structure, the localization of the orbitals becomes more pronounced and, thus, the spatial overlap between these orbitals decreases even further (Figure 3).

Closer examination of Figure 2 shows that the potential energy curves of all excited states are parallel to the ground state, except for the S_4 state of the planar keto-isomer with a vertical excitation energy of 3.8 eV at RI-CC2 level of theory. This state does exhibit a minimum at the twisted geometry at a dihedral angle of practically 90° . In the molecular orbital picture, this state is best represented by an electronic transition from the HOMO to the LUMO + 1 (not shown). While at the planar geometry of the keto-isomer, the orbitals are mainly localized on the keto side of P. Y. 101; they still do extend slightly over to the other ring. However, upon twisting, the HOMO and LUMO + 1 strictly localize on the keto side. Therefore, the S_4 state of the planar keto-isomer can be classified as a local excitation on that naphthalene ring where the proton has been transferred and which now possesses the keto group. As we will see later, this state seems to disappear from the low-energy region at the TDDFT/BP86 and TDDFT/B3LYP levels of theory and is only found when the BHLYP xc-functional is employed (Figure 4).

Twisting P. Y. 101 at the TDDFT Level of Theory Using Standard xc-Functionals. Let us now turn to the detailed investigation of how time-dependent density functional theory performs in the description of the potential energy surface of the S_1 state of P. Y. 101 along the twisting coordinate when standard local and hybrid xc-functionals are used. As noticed previously,³⁸ employing the BP86 xc-functional TDDFT generates a spurious minimum on the S_1 surface corresponding to the twisted geometry with a CNNC dihedral angle of 90° (upper panel in Figure 4). At that level of theory, the twisted geometry is 0.25 eV lower in energy than the planar trans keto-form of P. Y. 101. Comparison of the potential energy curve of the S_1 state of P. Y. 101 computed at the TDDFT/BP86 level with those obtained at the RI-CC2 level (Figure 2) suggests that S_1 may correspond to the state previously denoted as S_4 at the RI-CC2 level, since their corresponding curves exhibit practically identical shapes. However, this is not the case. Inspection of the HOMO and the LUMO orbitals involved in the S_1 state at the TDDFT/BP86 level (Figure 5) shows that they are practically identical to the ones employed in the RI-CC2 calculation, and thus, the S_1 state is the same state at TDDFT/BP86 as well as at the RI-CC2 level. Thus, it is not the ordering of the states that changes, but rather, it is the shape of the potential energy curves.

Naturally, the question arises why the shape of the S_1 potential energy curve changes so drastically from RI-CC2 to TDDFT/BP86. As we have mentioned before, this is most likely due to the CT failure of TDDFT when standard local xc-functionals are employed. A first indication is the increase

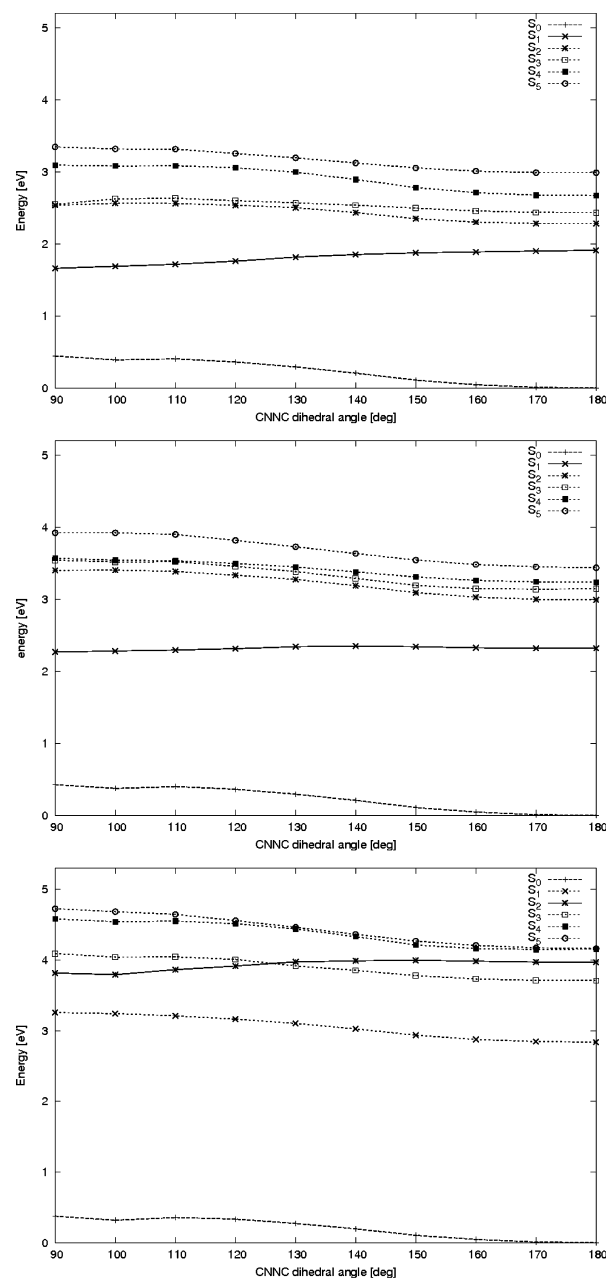


Figure 4. Potential energy curves of the ground and energetically lowest five excited singlet states calculated at the theoretical levels of TDDFT using the BP86 (top), B3LYP (middle), and BHLYP (bottom) xc-functionals along the dihedral angle of the central CNNC bisazomethine subunit of P. Y. 101.

of the excited state dipole moment along the twisting coordinate from about 10 D to more than 16 D, pointing at a rise of the charge transfer character. In principle, this is not unusual, since twisted intramolecular charge transfer (TICT) states have been found to exist in a plethora of aromatic push–pull systems. (See, for example, refs 47 and 48.) However, here in P. Y. 101, this twisting is undoubtedly an artifact, since the twisted structure corresponds to a transition state and not to a local minimum at the level of RI-CC2, our benchmark method.

A general simple procedure to disguise the CT failure is to use xc-functionals with an increasing amount of nonlocal Hartree–Fock (HF) exchange, since this gradually alleviates

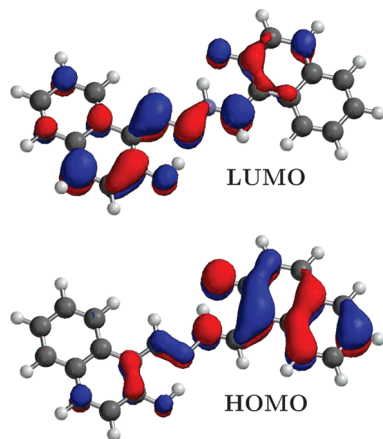


Figure 5. Highest occupied and lowest unoccupied molecular orbital of the planar keto-form of P. Y. 101 at the theoretical level of DFT/BP86.

the problem. Therefore, we have recomputed the potential energy curve of the S_1 state along the twisting coordinate also using the B3LYP and BHLYP xc-functionals which contain a constant amount of 20% and 50% HF exchange, respectively. As can be seen in the middle of Figure 4, the shape of the S_1 curve does indeed change when the B3LYP xc-functional is employed in the calculation of the twisting path. The S_1 curve is much flatter with the twisted and the planar structure being practically degenerate at the level of TDDFT/B3LYP. The twisted structure, however, is still slightly lower in energy than the planar one by only 0.05 eV. As a consequence, an unconstrained geometry optimization at the TDDFT/B3LYP level of theory converges onto the artificially twisted geometry. It is important to emphasize that the S_1 state is the same at TDDFT/BP86 and TDDFT/B3LYP: both correspond essentially to HOMO to LUMO transitions with the orbitals being indistinguishable (not shown).

Increasing the amount of HF exchange even further to 50%, i.e., using the BHLYP xc-functional in the TDDFT calculation of the twisting path, the potential curve of the S_1 state changes again. In the lower panel of Figure 4, it is seen that at the level of TDDFT/BHLYP the twisted minimum has disappeared and is now a transition state, as in RI-CC2, lying 0.41 eV above the planar keto-form of P. Y. 101. The obtained picture of the potential energy curves of the lowest excited electronic states at the level of TDDFT/BHLYP agrees qualitatively quite nicely with the one obtained with our benchmark method RI-CC2. Again, the S_1 state is the same at all levels of theory employed, and the potential energy surfaces have been computed along the same twisting path optimized at the level of TDDFT/BP86. Owing to the gradual removal of the local minimum corresponding to the twisted geometry with increasing amounts of nonlocal HF exchange, it can be undoubtedly concluded that the artificial twisted minimum on the S_1 surface of P. Y. 101 at the TDDFT/BP86 and TDDFT/B3LYP levels originates solely from the CT failure.

Nevertheless, the experimental absorption spectrum of P. Y. 101 is reasonably well reproduced using TDDFT/BP86 when the computed excitation energies are shifted by 0.41

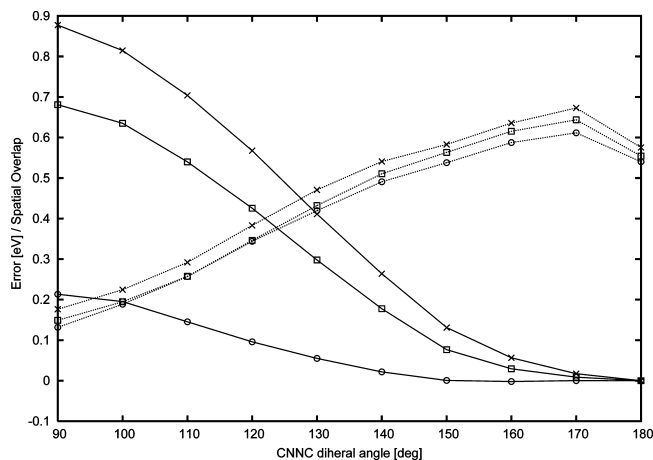


Figure 6. Comparison of the errors of the potential energy curves (solid lines) with the spatial overlap Δ of the involved orbitals at the TDDFT level employing the BP86 (crosses), B3LYP (boxes), and BHLYP (circles) xc-functionals along the twisting coordinate of P. Y. 101. For the definition of the error, see text.

eV to higher energies to correct for errors in the method and solution effects.^{8,36} In fact, comparison with experimental absorption spectra is very often the only possibility to validate the employed theoretical method, in particular when the molecules under investigation are too large for proper benchmark calculations. Furthermore, the computational effort is smaller for local GGA xc-functionals than for hybrid functionals, since for the latter also the HF exchange contribution needs to be evaluated. For very large molecules or molecular assemblies, this may make a significant difference. In such situations, an intrinsic diagnostic is very useful that helps to judge the influence of the CT failure and to estimate the quality of excitation energies or potential energy surfaces obtained with TDDFT. The Δ parameter as defined in the Introduction and explained in more detail in ref 31 is a useful measure of charge transfer character of an excited state and, thus, a useful diagnostic of the reliability of TDDFT calculations. Here, we have computed the value of Δ for the relevant S_1 state along the twisting coordinate, i.e., along the central CNNC dihedral angle of the bisazomethine unit for all three applied xc-functionals BP86, B3LYP, and BHLYP (Figure 6). The spatial overlap of the orbitals involved in the S_1 transition drops significantly from the planar to the twisted structure at all levels of theory in a practically identical way from a value of about 0.7 to below 0.2. The overall decrease of Δ , i.e., the reduction of spatial orbital overlap, demonstrates the increase in charge transfer character of the S_1 state along the twisting coordinate, which is in agreement with our previous observation that the static dipole moment of the S_1 state increases significantly upon twisting.

Also plotted in Figure 6 is the deviation of the TDDFT potential energy curves from the RI-CC2 curves for the different xc-functionals. For the calculation of the error, the energy of the planar keto-form is set to zero for all curves and the difference between the CC2 curve and the corresponding TDDFT curve defines the error. Despite the similar behavior of Δ for the three functionals, the error in the

Table 1. Comparison of the Absolute Excitation Energies of the Five Lowest Excited States Obtained at the RI-CC2 Level with Those Calculated by TDDFT Employing Different xc-Functionals at the Planar Structure of the Keto-Form of P.Y. 101 and at the Twisted Structure^a

state	RI-CC2	BP86	B3LYP	BHLYP	LC-BOP	ω PBE	ω B97X	CAM-B3LYP
planar keto-form (180°)								
S ₁	2.58 (0.84)	1.90 (0.29) [−0.68]	2.30 (0.51) [−0.28]	2.82 (0.80) [+0.24]	2.90 (0.85) [+0.32]	2.81 (0.83) [+0.23]	2.96 (0.86) [+0.38]	2.77 (0.80) [+0.19]
S ₂	3.32 (0.00)	2.27 (0.00) [−1.05]	2.97 (0.36) [−0.35]	3.68 (0.22) [+0.36]	3.75 (0.10) [+0.43]	3.64 (0.05) [+0.32]	3.80 (0.11) [+0.48]	3.63 (0.17) [+0.31]
S ₃	3.55 (0.15)	2.42 (0.27) [−1.13]	3.12 (0.00) [−0.33]	3.94 (0.03) [0.39]	3.80 (0.00) [+0.25]	3.67 (0.08) [+0.12]	3.97 (0.00) [+0.42]	3.76 (0.00) [+0.21]
S ₄	3.79 (0.01)	2.65 (0.21) [−1.14]	3.21 (0.03) [−0.58]	4.12 (0.00) [+0.34]	4.22 (0.33) [+0.43]	4.08 (0.07) [+0.29]	4.27 (0.31) [+0.48]	3.94 (0.02) [+0.15]
S ₅	3.96 (0.21)	2.97 (0.60) [−0.99]	3.41 (0.01) [−0.55]	4.13 (0.16) [+0.17]	4.35 (0.02) [+0.39]	4.11 (0.22) [+0.15]	4.40 (0.03) [+0.44]	4.06 (0.24) [+0.10]
twisted keto-form (90°)								
S ₁	2.80 (0.01)	1.21 (0.00) [−1.59]	1.83 (0.00) [−0.97]	2.86 (0.00) [+0.06]	3.38 (0.57) [+0.58]	3.10 (0.00) [+0.30]	3.43 (0.60) [+0.63]	2.90 (0.00) [+0.10]
S ₂	3.15 (0.55)	2.08 (0.06) [−1.07]	2.95 (0.00) [−0.20]	3.42 (0.85) [+0.27]	3.44 (0.07) [+0.29]	3.34 (0.61) [+0.19]	3.52 (0.06) [+0.37]	3.33 (0.61) [+0.18]
S ₃	3.48 (0.11)	2.09 (0.01) [−1.39]	3.09 (0.28) [−0.39]	3.69 (0.04) [+0.21]	3.70 (0.04) [+0.22]	3.61 (0.05) [+0.13]	3.76 (0.04) [+0.28]	3.60 (0.05) [+0.12]
S ₄	3.70 (0.00)	2.63 (0.01) [−1.07]	3.12 (0.29) [−0.58]	4.18 (0.19) [+0.48]	4.00 (0.00) [+0.30]	3.91 (0.00) [0.21]	4.15 (0.00) [+0.45]	4.01 (0.00) [+0.31]
S ₅	4.01 (0.24)	2.88 (0.38) [−1.13]	3.47 (0.00) [−0.54]	4.32 (0.01) [+0.31]	4.21 (0.55) [+0.20]	4.10 (0.21) [+0.09]	4.25 (0.24) [+0.24]	4.08 (0.20) [+0.07]

^a Excitation energies are given in eV, oscillator strengths are given in parentheses, and the difference to the RI-CC2 reference value is given in eV in square brackets.

potential energy curves is significantly different. For the BP86 xc-functional, the error increases drastically along the twisting coordinate and reaches a value of 0.88 eV at the twisted geometry. In other words, at the twisted geometry, the excitation energy of the S₁ state is strongly underestimated by that value, in contrast to the planar structure. This underestimation of the excitation energy at a particular geometry as observed here for TDDFT/BP86 introduces spurious minima on excited state potential energy surfaces. For B3LYP, the error increase is generally smaller due to its 20% nonlocal HF exchange, which partially corrects for the CT failure. The error in the potential energy surface at the twisted geometry amounts to 0.69 eV, i.e., 0.2 eV less than at the BP86 level, although the spatial overlap of the involved orbitals is in analogy to BP86 below 0.2. Using BHLYP finally improves the situation substantially. The inclusion of 50% HF exchange leads to a decrease of the error at the twisted geometry to only 0.21 eV. Again, the spatial overlap is unaffected by the inclusion of HF exchange. In this series, BHLYP is the only xc-functional that yields the qualitatively correct shape of the potential energy surface, however, still with a small bias toward twisted structures with large charge transfer character.

Let us briefly return to the electronic state which was found as S₄ at the RI-CC2 level of theory (Figure 2) which exhibits a minimum at the twisted geometry. We have proven above that the S₁ state is indeed the same state at all employed levels of TDDFT and RI-CC2 although the shapes of the curves are remarkably different. However, no other states of those displayed at the TDDFT/BP86 and TDDFT/B3LYP levels exhibit a potential energy curve similar to the one of the S₄^{CC2} state except S₁. At TDDFT/BHLYP, the S₄^{CC2} state reappears as S₃ at the planar geometry and corresponds also to the HOMO to LUMO + 1 electronic transition. Note that

the orbitals do not change in the valence region, so the HOMO − 1, HOMO, LUMO, and LUMO + 1 are virtually identical at all employed levels of theory. Naturally, one may, thus, ask the question, if S₁ does not correspond to S₄^{CC2} where is this state at the TDDFT/BP86 and TDDFT/B3LYP levels? In fact, the corresponding state does exist, but it is not found among the five lowest excited states displayed in Figure 4. This has again to do with the CT failure of TDDFT and the artificial lowering of the excitation energies of CT excited states compared to locally excited states as the S₄ state. With decreasing amount of HF exchange from BHLYP to BP86, more and more CT excited states drop below the locally excited S₄^{CC2} state making this state seemingly disappear.

Comparison of the absolute excitation energies (Table 1) obtained at BP86, B3LYP and BHLYP show the typical trend to higher excitation energies. For example, the S₁ state possesses an excitation energy of 1.90 eV at the TDDFT/BP86 level and 2.30 and 2.82 eV using the B3LYP and BHLYP xc-functionals, respectively. This is a well-known phenomenon directly related to the amount of nonlocal Hartree–Fock exchange and the concomitant increase of the occupied-virtual gap. Much more interesting, however, is the absolute error of all states compared to our theoretical benchmark RI-CC2 results. If the error of all computed states is roughly the same, one can reliably compute absorption spectra and investigate excited state processes, in which more than one electronic state is involved. For the latter, precise knowledge of state crossings or conical intersection, i.e., of the relative position of the involved states, is an inevitable prerequisite. As is easily seen in Table 1, the deviations of the BP86 excitation energies of the S₁–S₅ states cover a wide range from −0.68 up to −1.23 eV at the planar geometry and −1.07 to −1.59 eV at the twisted geometry revealing

an unbalanced treatment of the different excited states of P.Y. 101. The situation is slightly improved for the B3LYP xc-functional; here, the absolute deviation is smaller at the planar geometry (-0.28 to -0.58 eV), and the shift is similar for all states. Although the deviation from the RI-CC2 results is still a bit large, the quality of the states is roughly the same for all resulting in a more balanced treatment. However, at the twisted geometry, the quality of the B3LYP results degrades strongly and the deviation from the RI-CC2 results becomes as large as -0.97 eV for the S_1 state due to its increased CT character leading to an unbalanced treatment of the states. The situation is greatly improved when the BHLYP xc-functional is employed within TDDFT. The deviation from the RI-CC2 results ranges from $+0.17$ to $+0.48$ eV, slightly overestimating the excitation energies, but most importantly, the quality of the results does not decrease at the twisted geometry of P.Y. 101. The deviation of the S_1 state is here actually the smallest with only 0.06 eV due to the tendency to underestimate excitation energies of CT states compensating the general overestimation of the excitation energies by BHLYP.

Twisting P. Y. 101 at the TDDFT Level of Theory Using Long-Range Separated xc-Functionals. In the previous section, we have seen that inclusion of at least 50% long-range Hartree–Fock exchange, as in BHLYP, largely corrects for the false shape of the potential energy surface of the S_1 state of P.Y. 101 along the twisting coordinate when local and GGA xc-functionals are employed with TDDFT. Using BHLYP, the PES exhibits correctly a transition state at a 90° dihedral angle and not a local minimum (Figure 4). However, BHLYP still has a bias to favor charge transfer (Figure 6) and, in addition, it overestimates excitation energies generally by about 0.2–0.5 eV as compared to RI-CC2, which has been observed to be generally the case. Recently, long-range separated (LRS) xc-functionals have been suggested and designed to also correct for the charge transfer failure of local and GGA xc-functionals in TDDFT. They do not contain a constant fraction of nonlocal Hartree–Fock exchange but instead use an increasing amount with growing electron–electron distance. While most LRS-functionals include at long-range 100% HF exchange, CAM-B3LYP for instance reaches only 65%. Thereby, functionals including 100% exact orbital exchange do by construction correctly describe the $1/R$ dependence of potential energy curves of long-range charge transfer excited states along a charge-separation coordinate R at the TDDFT level, and the longer-ranged the CT the better. LRS-functionals with lower fractions of HF exchange recover only the corresponding lower fraction of the $1/R$ asymptote.¹¹ However, it has not been investigated and compared yet, how different LRS-functionals perform in the description of intramolecular charge transfer problems. For this objective, the investigated twisting coordinate of the keto-form of P.Y. 101 is a perfect test case. On one hand, at the planar configuration with a central bisazomethine dihedral angle of 180° , only little nonlocal Hartree–Fock is needed to obtain reasonable excitation energies and reliable spectra, for example B3LYP would be sufficient (Table 1), while on the other hand increasing amounts of Hartree–Fock exchange are required

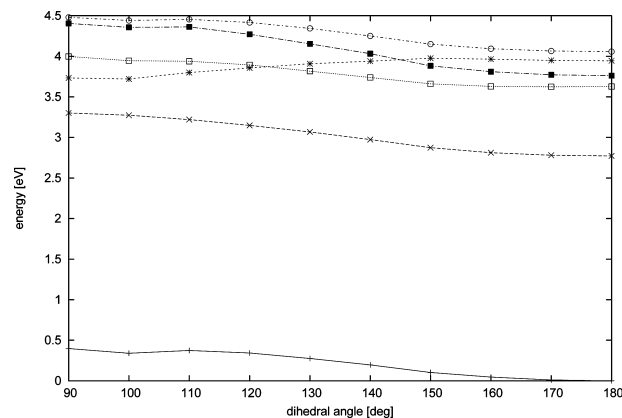


Figure 7. Potential energy curves of the ground and energetically lowest five excited singlet states calculated at the theoretical level of TDDFT using the long-range separated xc-functional CAM-B3LYP along the dihedral angle of the central CNNC bisazomethine subunit of P. Y. 101.

to describe the potential energy surface correctly, more than 50%, since BHLYP is still favoring charge transfer (Figure 6). Therefore, we have computed the potential energy surfaces of the five energetically lowest excited states along the twisting coordinate of P.Y. 101 using the LRS-functionals LC-BOP,^{17–19} ω PBE,^{20,21} ω B97X,^{22,23} and CAM-B3LYP¹⁶ in strict analogy to the calculations reported above. The curves obtained with all these LRS-functionals are very similar with minor deviations in the absolute energies; the overall qualitative picture, however, is practically identical. As one example, the CAM-B3LYP curves are displayed in Figure 7. Comparison with the computed curves at RI-CC2 (Figure 2) and TDDFT/BHLYP (lowest panel of Figure 4) reveals an excellent agreement. As it was the case for all tested xc-functionals so far, BP86, B3LYP, and BHLYP, the spatial overlap of the molecular orbitals involved in the S_1 state measured by the Λ -parameter decreases also for CAM-B3LYP from 0.65 to 0.15, indicating an increasing CT character of S_1 along the twisting coordinate.

For a detailed analysis of the performance of the various LRS-functionals with respect to the correct description of the shape of the potential energy surface of the critical S_1 state along the twisting coordinate, we have again compared it to the potential energy curve at the RI-CC2 level in analogy to above. The differences between the potential energy curves at the TDDFT level employing the LRS-functionals and RI-CC2 are plotted in Figure 8; a positive sign of the error corresponds to an underestimation of the energy of the twisted form, and a negative one corresponds to an overestimation. As can be seen, the deviations from the RI-CC2 curve are much smaller for all LRS-functionals than for BP86 or B3LYP and are of the same order of magnitude as the deviation of the BHLYP curve, i.e., at most 0.2 eV at the twisted structure of P. Y. 101 which exhibits pronounced charge transfer character. While CAM-B3LYP has a small tendency to underestimate the energy of the twisted charge transfer structure relative to the planar one by as little as 0.1 eV, all other LRS-functionals overestimate its energy. This is probably related to the fact that CAM-B3LYP includes only 65% or long-range HF exchange, while all other tested

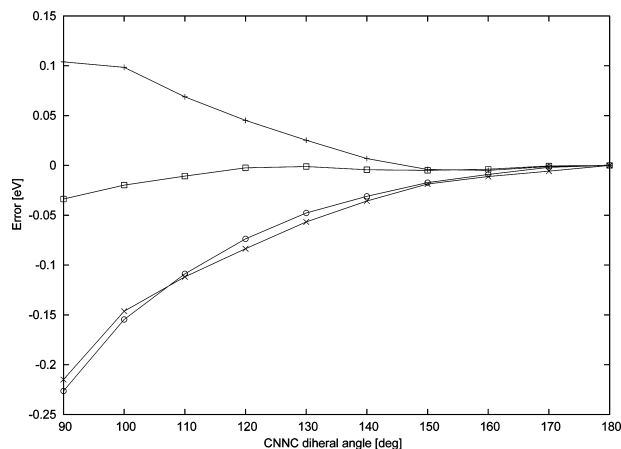


Figure 8. Errors of the potential energy curves of the S_1 state of P. Y. 101 along the twisting coordinate at the TDDFT level employing the long-range separated xc-functionals LC-BOP (circles), ω B97X (crosses), ω PBE (boxes), and CAM-B3LYP (pluses) relative to the curve calculated at RI-CC2 level. For a detailed definition of the error see text.

LRS-functionals include 100%. Both LC-BOP and ω B97X overestimate the excitation energy of the twisted charge transfer structure by about 0.22 eV relative to the planar keto-form of P. Y. 101, i.e., they overcompensate the charge transfer failure of TDDFT and shift excitation energies of charge transfer states potentially to too high values. However, the curve computed with ω PBE deviates only as little as 0.03 eV from RI-CC2 and yields a practically identical curve. However, the observed deviations of the curves are small, in particular the ones of CAM-B3LYP and ω PBE, and lie clearly within the error of the applied TDDFT method. In fact, using LRS-functionals prevents the overemphasizing charge transfer character as the conventional GGA xc-functionals or hybrids with low fractions of HF exchange do.

Let us finally turn to the absolute errors in the excitation energies of the five lowest excited states, where again the RI-CC2 results serve as a benchmark. Here, it is again important to emphasize that a consistent treatment of all excited states is of particular importance for reliable calculation of absorption spectra and excited state dynamics. Thus, it is desirable that one functional exhibits the same quality for all energetically low-lying states. The vertical excitation energies of the five energetically lowest electronic states S_1 to S_5 of the planar and twisted structure of the keto-form of P. Y. 101 computed using TDDFT and the various LRS-functionals are compiled in Table 1.

LC-BOP and ω B97X reach about the same level of accuracy, which is also the same for BHLYP, as they deviate consistently by +0.2 to +0.6 from the RI-CC2 values, i.e., the computed excitation energies at those TDDFT levels are consistently too high. The above noticed tendency of LC-BOP and ω B97X to shift CT states to too high excitation energies is also seen here, since their deviation from the RI-CC2 results increases from +0.3 eV to +0.6 eV upon twisting, i.e., with increase of CT character. The two xc-functionals that yield the best agreement with the RI-CC2 results and which describe all tested excited states at the

planar as well as twisted structure of P. Y. 101 in the most balanced way are CAM-B3LYP and ω PBE. While CAM-B3LYP has a slightly better agreement in the absolute values of the excitation energies, ω PBE treats the excited states of the twisted and planar structures in a slightly more balanced way. However, these deviations are very small and are much smaller than the typical errors of TDDFT excitation energies.

Summary and Conclusions

It has been noticed previously that local, GGA, and hybrid xc-functionals cannot describe the potential energy curve of the S_1 state of Pigment Yellow 101 (P. Y. 101) along a twisting coordinate of the central bisazomethine subgroup. The increasing intramolecular CT character of the S_1 state along this coordinate leads to an underestimation of the energy of the twisted configuration relative to the planar one, resulting in an artificial twisted minimum on its potential energy surface.

Here, the potential energy curves of the five energetically lowest excited states have been recomputed along this coordinate employing TDDFT with various xc-functionals ranging from the standard hybrid-functionals B3LYP and BHLYP up to modern long-range separated (LRS) xc-functionals LC-BOP, ω B97X, ω PBE, and CAM-B3LYP. The obtained results are evaluated with respect to RI-CC2 computations, which serve as our benchmark. Furthermore, a newly introduced diagnostic Λ parameter to measure the degree of CT character of a particular state has been employed to relate the failure of the standard functionals to the spatial overlap of the molecular orbitals involved in the electronic transition.

Using a series of TDDFT calculations employing the BP86, B3LYP, and BHLYP xc-functionals with increasing amounts of Hartree–Fock exchange, we could unequivocally demonstrate that the problems in the description of the S_1 surface arise from the CT failure of TDDFT. Furthermore, the Λ parameter is a very useful instrument to identify problematic CT cases for TDDFT, since the overlap of the involved orbitals and, thus, Λ decreases smoothly with the increasing error along the twisting coordinate. It is also seen that BHLYP largely alleviates the CT problem for P. Y. 101; however, this xc-functional still has a bias toward underestimating energies of CT states.

The situation is greatly improved when LRS-functionals are employed. While ω B97X and LC-BOP tend to overcorrect for the CT failure of TDDFT and yield the twisted structure at slightly too high energies, ω PBE and CAM-B3LYP yield potential energy surfaces for the S_1 state in excellent agreement with the RI-CC2 curve. The LRS-functionals consistently overestimate the vertical excitation energies of the five energetically lowest excited states, CAM-B3LYP and ω PBE by only 0.1–0.3 eV, the latter again in excellent agreement with the RI-CC2 values. On the basis of these findings, one can undoubtedly recommend LRS-functionals, preferably CAM-B3LYP and ω PBE, to be used in the calculation of excited states of molecules with certain intramolecular charge transfer character. For P. Y. 101 and similar cases, BHLYP also

yields qualitatively correct potential energy curves and reasonably balanced values for the energetically low lying excited states but still with a small bias to underestimate the energy of CT states.

Finally, it is important to note that P. Y. 101 is just one example for which the different xc-functionals have been evaluated. However, it is particularly representative since the electronic structure of excited states usually does change along a reaction coordinate, sometimes quite drastically and very often the amount of charge transfer changes substantially. For instance, this is the case in all twisted intramolecular charge transfer (TICT) systems, for which dimethylaminobenzonitrile (DMABN) is the proto-typical example. Indeed, the findings of the present study concerning Λ and the performance of LRS-functionals are fully consistent with the DMABN study of ref 34. Therefore, the observed trends can be expected to be valid for most other systems as well, but it might well be that the relative performance of the LRS-functionals may be different. A thorough evaluation of the performance of standard xc- or LRS-functionals and of the quality of the results obtained with TDDFT is, thus, strongly recommended or even demanded.

Another critical note concerns the chosen RI-CC2 method as the benchmark. For the molecular system under investigation and the chosen problem of intramolecular charge transfer, the RI-CC2 method is certainly adequate, since all states are undoubtedly single excitations. However, it has been demonstrated recently that the overall error in excitation energies is about the same for RI-CC2 and TDDFT calculations once LRS xc-functionals are employed,⁴⁹ which is essentially the same result that we observe here for the PES of P.Y.101. It is also well-known that RI-CC2 does not systematically provide more accurate results than TDDFT, but of course the qualitative evolution of excitation energies and transition moments is better reproduced by RI-CC2.^{49–51} At present, other ab initio computations with higher accuracy are not feasible for the excited states of P. Y. 101 due to its molecular size. One could have chosen a smaller model test system, but we wanted to demonstrate the applicability and the usefulness of the Λ -parameter and available LRS-functionals for the investigation of a real chemical system.

Acknowledgment. Andreas Dreuw acknowledges financial support by the Deutsche Forschungsgemeinschaft as a Heisenberg-Professor. This project is funded within the Priority Programme SPP1145 of the Deutsche Forschungsgemeinschaft. Computation time has been generously provided by the Center of Scientific Computing of the Goethe University of Frankfurt/Main.

References

- (1) Runge, E.; Gross, E. K. U. *Phys. Rev. Lett.* **1984**, *52*, 997.
- (2) Casida, M. E. In *Recent Advances in Density Functional Methods, Part I*; Chong, D. P., Ed.; World Scientific: Singapore, 1995; pp 155–192.
- (3) Dreuw, A.; Head-Gordon, M. *Chem. Rev.* **2005**, *105*, 4009.
- (4) Hay, P. J. *J. Phys. Chem. A* **2002**, *106*, 1634.
- (5) Nazeeruddin, M. K.; De Angelis, F.; Fantacci, S.; Selloni, A.; Viscardi, G.; Liska, P.; Ito, S.; Takeru, B.; Grätzel, M. *J. Am. Chem. Soc.* **2005**, *127*, 16835.
- (6) Dreuw, A. *Chem. Phys. Chem.* **2006**, *7*, 2259.
- (7) Suramitr, S. P. W.; Meeto, W.; Hannongbua, S. *Theor. Chem. Acc.* **2010**, *125*, 35.
- (8) Dreuw, A.; Plötner, J.; Lorenz, L.; Wachveitl, J.; Djanhan, J. E.; Brüning, J.; Bolte, M.; Schmidt, M. U. *Ang. Chem. Int. Ed.* **2005**, *44*, 7783.
- (9) Diercks, M.; Grimme, S. *J. Chem. Phys.* **2004**, *120*, 3544.
- (10) Tozer, D. J.; Amos, R. D.; Handy, N. C.; Roos, B. J.; Serrano-Andres, L. *Mol. Phys.* **1999**, *97*, 859.
- (11) Dreuw, A.; Weisman, J. L.; Head-Gordon, M. *J. Chem. Phys.* **2003**, *119*, 2943–2946.
- (12) Dreuw, A.; Head-Gordon, M. *J. Am. Chem. Soc.* **2004**, *126*, 4007–4016.
- (13) Sobolewski, A. L.; Domcke, W. *Chem. Phys.* **2003**, *294*, 73.
- (14) Perdew, J. P.; Parr, R. G.; Levy, M.; Balduz, J. L., Jr. *Phys. Rev. Lett.* **1982**, *49*, 1691.
- (15) Tozer, D. J. *J. Chem. Phys.* **2003**, *119*, 12697.
- (16) Yanai, T.; Tew, D. P.; Handy, N. C. *Chem. Phys. Lett.* **2004**, *393*, 51.
- (17) Tawada, Y.; Tsuneda, T.; Yanagisawa, S.; Yanai, T.; Hirao, K. *J. Chem. Phys.* **2004**, *1210*, 8425.
- (18) Sato, T.; Tsuneda, T.; Hirao, K. *J. Chem. Phys.* **2007**, *126*, 234114.
- (19) Chiba, M.; Tsuneda, T.; Hirao, K. *J. Chem. Phys.* **2006**, *124*, 144106.
- (20) Rohrdanz, M. A.; Herbert, J. M. *J. Chem. Phys.* **2008**, *129*, 034107.
- (21) Rohrdanz, M. A.; Martins, K. M.; Herbert, J. M. *J. Chem. Phys.* **2009**, *130*, 054112.
- (22) Chai, J.-D.; Head-Gordon, M. *J. Chem. Phys.* **2008**, *128*, 084106.
- (23) Chai, J.-D.; Head-Gordon, M. *Phys. Chem. Chem. Phys.* **2008**, *10*, 6615.
- (24) Vydrov, O. A.; Heyd, J.; Krukau, A. V.; Scuseria, G. E. *J. Chem. Phys.* **2006**, *125*, 074106.
- (25) Vydrov, O. A.; Scuseria, G. E. *J. Chem. Phys.* **2006**, *125*, 234109.
- (26) Baer, R.; Neuhauser, D. *Phys. Rev. Lett.* **2005**, *94*, 043002.
- (27) Stein, T.; Kronik, L.; Baer, R. *J. Am. Chem. Soc.* **2009**, *131*, 2818.
- (28) Görling, A. *Phys. Rev. Lett.* **1999**, *83*, 5459.
- (29) Ivanov, S.; Hirata, S.; Bartlett, R. J. *Phys. Rev. Lett.* **1999**, *83*, 5455.
- (30) Gimon, T.; A, I.; Heßelmann, A.; Görling, A. *J. Chem. Theory Comput.* **2009**, *5*, 781.
- (31) Peach, M. J. G.; Benfield, P.; Helgaker, T.; Tozer, D. J. *J. Chem. Phys.* **2008**, *128*, 044118.
- (32) Peach, M. J. G.; Le Sueur, C. R.; Ruud, K.; Guillaume, M.; Tozer, D. J. *Phys. Chem. Chem. Phys.* **2009**, *11*, 4465.
- (33) Peach, M. J. G.; Tozer, D. J. *J. Mol. Struct.: Theochem.* **2009**, *914*, 110.

- (34) Wiggins, P.; Williams, J. A. G.; Tozer, D. J. *J. Chem. Phys.* **2009**, *131*, 091101.
- (35) Dwyer, A. D.; Tozer, D. J. *Phys. Chem. Chem. Phys.* **2010**, *12*, 2816.
- (36) Plötner, J.; Dreuw, A. *Phys. Chem. Chem. Phys.* **2006**, *8*, 1197.
- (37) Lorenz, L.; Matyilsky, V.; Plötner, J.; Dreuw, A.; Wachtveitl, J. *J. Phys. Chem. A* **2007**, *111*, 10891.
- (38) Plötner, J.; Dreuw, A. *Chem. Phys.* **2008**, *347*, 472.
- (39) Becke, A. D. *J. Chem. Phys.* **1993**, *98*, 5648.
- (40) Lee, C.; Yang, W.; Parr, R. G. *Phys. Rev. B* **1988**, *37*, 785.
- (41) Becke, A. D. *J. Chem. Phys.* **1993**, *98*, 1372.
- (42) Haettig, C.; Weigend, F. *J. Chem. Phys.* **2000**, *113*, 5154.
- (43) Kong, J.; et al. *J. Comput. Chem.* **2000**, *21*, 1532.
- (44) TURBOMOLE Version 5.7.1.
- (45) DALTON, a molecular electronic structure program, Release 2.0; 2005; see <http://daltonprogram.org/>.
- (46) Christiansen, O.; Koch, H.; Jørgensen, P.; Helgaker, T. *Chem. Phys. Lett.* **1996**, *263*, 530.
- (47) Grabowski, Z. R.; Rotkiewicz, K.; Rettig, W. *Chem. Rev.* **2003**, *103*, 3899.
- (48) Zakharov, M.; Krauss, O.; Nosenko, Y.; Brutschy, B.; Dreuw, A. *J. Am. Chem. Soc.* **2009**, *131*, 461.
- (49) Jacquemin, D.; Wathelet, V.; Perpète, E. A.; Adamo, C. *J. Chem. Theory Comput.* **2009**, *5*, 2420.
- (50) Caricato, M.; Trucks, G. W.; Frisch, M. J.; Wiberg, K. B. *J. Chem. Theory Comput.* **2010**, *6*, 370.
- (51) Silva-Junior, M. R.; Schreiber, M.; Sauer, S. P. A.; Thiel, W. *J. Chem. Phys.* **2008**, *129*, 104103.

CT1001973